

## RESEARCH ARTICLE

# Proteomic analysis of *Aspergillus nidulans* cultured under hypoxic conditions

Motoyuki Shimizu, Tatsuya Fujii, Shunsuke Masuo, Kensaku Fujita and Naoki Takaya

Graduate School of Life and Environmental Sciences, University of Tsukuba, Tsukuba, Ibaraki, Japan

The fungus *Aspergillus nidulans* reduces nitrate to ammonium and simultaneously oxidizes ethanol to acetate to generate ATP under hypoxic conditions in a mechanism called ammonia fermentation (Takasaki, K. *et al. J. Biol. Chem.* 2004, 279, 12414–12420). To elucidate the mechanism, the fungus was cultured under normoxic and hypoxic (ammonia fermenting) conditions, intracellular proteins were resolved by 2-DE, and 332 protein spots were identified using MALDI MS after tryptic digestion. Alcohol and aldehyde dehydrogenases that play key roles in oxidizing ethanol were produced at the basal level under hypoxic conditions but were obviously provoked by ethanol under normoxic conditions. Enzymes involved in gluconeogenesis, as well as the tricarboxylic and glyoxylate cycles, were downregulated. These results indicate that the mechanism of fungal energy conservation is altered under hypoxic conditions. The results also showed that proteins in the pentose phosphate pathway as well as the metabolism of both nucleotide and thiamine were upregulated under hypoxic conditions. Levels of xanthine and hypoxanthine, deamination products of guanine and adenine were increased in DNA from hypoxic cells, indicating an association between hypoxia and intracellular DNA base damage. This study is the first proteomic comparison of the hypoxic responses of *A. nidulans*.

Received: December 17, 2007

Revised: June 24, 2008

Accepted: July 11, 2008

**Keywords:**

*Aspergillus nidulans* / Hypoxia / Nucleotide metabolism / Protein expression

## 1 Introduction

Most eukaryotes inhabit a normoxic milieu. They absolutely require oxygen (O<sub>2</sub>) for growth since O<sub>2</sub> serves as a substrate for the biosynthesis of some essential compounds such as sterol and heme, and for O<sub>2</sub> respiration. For most eukaryotes,

O<sub>2</sub> respiration is a mitochondrial mechanism that is indispensable for conserving the energy required for growth. Oxygen depletion imposes a challenge upon eukaryotic cells, most of which respond to low O<sub>2</sub> tension and induce adaptation mechanisms for survival. Transcription factors affecting the expression of hypoxic genes participate in cellular metabolism, growth and death [1].

The eukaryote *Saccharomyces cerevisiae* expresses an alcohol (ethanol) fermentation mechanism under hypoxic conditions. This accompanies alterations of global transcription [2–4] and cellular proteins [5, 6] for energy conservation and for the biosynthesis of cellular components. For example, in response to anoxia (O<sub>2</sub> depletion) *S. cerevisiae* downregulates the genes for respiratory complexes and the tricarboxylic acid (TCA) cycle, and upregulates those for glycolysis and ethanol production [5]. Oxygen sensing and the regulation of O<sub>2</sub>-responsive genes by heme and sterols in yeast have been reported [7–9]. Except for extensive studies of yeast, the hypoxic responses of other fungi, especially those that are filamentous, remain obscure. Zhou *et al.* showed

**Correspondence:** Dr. Naoki Takaya, Graduate School of Life and Environmental Sciences, University of Tsukuba, 1-1-1 Tennodai, Tsukuba, Ibaraki 305-8572, Japan

**E-mail:** ntakeya@sakura.cc.tsukuba.ac.jp

**Fax:** +81-29-853-4937

**Abbreviations:** **Ack**, acetate kinase; **ADH**, alcohol dehydrogenase I; **ALDH**, aldehyde dehydrogenase; **BPB**, bromophenol blue; **CoA**, coenzyme A; **GABA**,  $\gamma$ -aminobutyrate; **GLOX**, glyoxylate; **NADP-GDH**, NADP<sup>+</sup>-dependent glutamate dehydrogenase; **PAPS**, phosphoadenosine 5-phosphosulfate; **PPP**, pentose-phosphate pathway; **TCA**, tricarboxylic acid; **THI4**, thiazole biosynthetic protein; **THI5**, pyrimidine biosynthetic protein; **TPP**, thiamine pyrophosphate

that the fungus *Fusarium oxysporum* reduces nitrate to ammonium under hypoxic conditions and simultaneously oxidizes ethanol to acetate. This reaction generates ATP through substrate-level phosphorylation, and is referred to as ammonia fermentation [10, 11]. Thereafter, we found that the fungus *Aspergillus nidulans* produced a similar reaction and identified *niaD* and *niiA*, which encode nitrate and nitrite reductases, as the enzymes responsible for ammonia production [12, 13]. We also found that the acetogenic reaction is catalyzed by alcohol dehydrogenase, coenzyme A (CoA)-acylating aldehyde dehydrogenase (ALDH) and acetate kinase (Ack). The last step of the reaction catalyzed by Ack produced ATP. The production of Ack requires a functional *facA* gene that encodes acetyl-CoA synthetase (ACS), which is widely conserved in both prokaryotes and eukaryotes [12]. The cellular response mechanisms of the fungus have not been documented in detail.

Proteomic differential display is a powerful tool for identifying proteins and studying global cellular responses to a specific environment. Recent progress in the genomic analysis of over 25 species of filamentous fungi has revealed nucleotide sequences of mostly complete sets of genes. These findings have enabled genomic and proteomic comparisons of these fungi, which should provide a greater insight into the cellular systems of eukaryotic microorganisms. Proteomic studies of several filamentous fungi have already begun [14–18]. The genome sequences of *A. nidulans*, *Aspergillus niger*, *Aspergillus oryzae*, *Aspergillus flavus*, and *Aspergillus fumigatus* have been published and proteomic osmoadaptation studies of *A. nidulans* have started [19]. Responses to antibiotics [20] and the iron regulation [21] of intracellular proteins have been studied in *A. nidulans*. Further proteomic comparisons should reveal how fungi adapt to various environments.

Here, we performed comparative proteomic analyses to understand the hypoxic responses of *A. nidulans* cells. Intracellular proteins were separated and identified using 2-DE and MALDI MS after in-gel tryptic digestion. We uncovered the global molecular events that occur in *A. nidulans* cells in response to hypoxia.

## 2 Materials and methods

### 2.1 Culture conditions

*A. nidulans* strain A26 (*biA1*) was obtained from the Fungal Genetic Stock Center (University of Kansas Medical Center). Conidia ( $10^8$ ) were transferred to 500 mL Erlenmeyer flasks containing 100 mL of MMDN (10 g/L fructose, 6 g/L  $\text{NaNO}_3$ , 10 mM  $\text{KH}_2\text{PO}_4$ , 7 mM KCl, 2 mM  $\text{MgSO}_4$ , 0.2% Hutner's trace metals v/v [12]) and normoxically incubated at 30°C for 20 h at 120 rpm (preculture). Resultant mycelia were collected by centrifugation, washed twice with 7 g/L NaCl, and then inoculated into 500 mL Erlenmeyer flasks containing 300 mL of MMEN (100 mM ethanol, 10 mM  $\text{NaNO}_3$ , 10 mM

$\text{KH}_2\text{PO}_4$ , 7 mM KCl, 2 mM  $\text{MgSO}_4$ , 0.2% Hutner's trace metals v/v). Biotin (0.2 µg/L) was added to all media. Head-space in the flasks was replaced with nitrogen gas by purging the air for 15 min, then the flasks were sealed with butyl rubber stoppers and rotated at 30°C at 120 rpm to induce ammonia fermentation. Normoxic conditions were maintained by agitating 100 mL of MMEN medium in flasks sealed with cotton plugs but without replacing the head space air.

### 2.2 Sample preparation for 2-DE

The mycelia were washed with chilled water, frozen under liquid nitrogen, ground into a fine powder using a mortar and pestle, dissolved in four volumes of cold acetone (−20°C) containing 10% TCA w/v, stored overnight at −20°C, and centrifuged at 15 000 × g for 15 min. The precipitate was washed twice with cold acetone containing 1% 2-mercaptoethanol v/v and air-dried for 5 min at room temperature. The pellet was dissolved in buffer containing 7 M urea, 2 M thiourea, 4% CHAPS w/v, 20 mM DTT, 1.0% IPG buffer v/v (pI 4–7 or pI 6–11, GE Healthcare) and a trace amount of bromophenol blue (BPB). Samples were incubated in the same buffer for 1 h at room temperature and insoluble material was removed by centrifugation at 20 000 × g for 10 min.

### 2.3 2-DE

Samples prepared from mycelia grown under normoxic and hypoxic conditions were isoelectrically focused in parallel with an IPGphor system (GE Healthcare). Proteins (200 µg) in urea buffer were loaded onto immobilized pI gradient strips (pI 4–7 or pI 6–11, 18 cm, GE Healthcare) and then the strips were rehydrated for 12 h. Proteins were isoelectrically focused as follows: 500 V for 1 h, 500–1000 V for 1 h, 1000–8000 V for 2 h, and 8000 V for 8 h. Thereafter, the strips were equilibrated with 6 M urea containing 130 mM DTT, 30% glycerol w/v, 2% SDS w/v, and a trace amount of BPB, and then with 6 M urea containing 135 mM iodoacetamide, 30% glycerol, 2% SDS, and a trace amount of BPB. The strips were loaded onto precast 11.0% homogenous polyacrylamide (slab) gels (PAGE) (20 cm × 20 cm). The lower and upper running buffers comprised 385 mM Tris containing 50 mM glycine and 0.1% SDS, with or without 0.2 g/L sodium azide, respectively and proteins were separated at 24 mA per gel. The slabs were immersed in 7% acetic acid v/v, 10% methanol v/v and then stained with SYPRO Ruby (BioRad, Hercules, CA, USA) by agitation at room temperature for 3 h. The gels were washed with 7% acetic acid, 10% methanol for 30 min and then protein spots were detected using a ChemiDoc XRS (BioRad). Gel images were loaded into the Proteomeweaver software (version 4.0, BioRad) and processing, spot detection, quantitation, gel matching, and warping proceeded according to the manufacturer's instructions [22]. The volumes of spots were nor-

malized by dividing the volume of each spot by sum of the total spot volume. All proteomic differential display experiments were independently repeated three times. Mean values of the normalized volumes from the three experiments determined the expression level of each protein, and were used for statistical tests (Student's *t*-test). We established the level of significance at  $p < 0.05$ .

## 2.4 In-gel tryptic digestion

Each target spot was excised with a clean scalpel, cut into 2 mm cubes, transferred into a clean 1.5 mL microcentrifuge tube, and washed with 40% 1-propanol v/v at room temperature for 15 min. The solvent was removed and the cubes were dehydrated in 200 mM ammonium bicarbonate in 50% ACN v/v at room temperature for 15 min. The dehydrated cubes were treated with a minimal volume of 20 ng/ $\mu$ L trypsin gold (Promega, Madison, WI, USA) in 100 mM ammonium bicarbonate for rehydration, chopped into four to five smaller pieces, and incubated at 37°C. After 12 h, the supernatant was collected, and the gel pieces were extracted once with 100 mM ammonium bicarbonate, and twice with 80% ACN containing 0.05% TFA v/v. The supernatant and the extracts were combined and concentrated to about 10  $\mu$ L using a SpeedVac centrifugal evaporator.

## 2.5 MALDI-TOF-MS analysis

Peptide mixtures (Section 2.4) were desalted using ZipTips C<sub>18</sub> (Millipore, Billerica, MA, USA), and then 2  $\mu$ L was loaded onto a target plate for MALDI-TOF-MS analysis. The solution was mixed with 1  $\mu$ L of 50% ACN v/v containing 10 mg/mL CHCA and 0.1% TFA w/v and then dried at room temperature. Mass spectra were obtained using an AXIMA mass spectrometer equipped with a 337 nm N<sub>2</sub> laser in the positive ion reflectron mode (Shimadzu, Kyoto, Japan). Spectral data were processed by averaging 128 spectra, each of which was obtained from independent laser firings. The mass of each peptide was calibrated against autolytic trypsin fragments as internal standards.

## 2.6 Identification of proteins

Proteins were identified by PMF analysis according to the molecular mass of each tryptic fragment and using the MASCOT (Matrix Science) search engines of the entire NCBI protein database and a protein sequence library constructed in-house with the most recent annotation of the *A. nidulans* genome (version 3, Broad Institute). Monoisotopic peptides and possible oxidation of methionine and carbamidomethylation of cysteine residues were considered for PMF analysis. A maximum of one missed tryptic cleavage *per* protein was allowed in the database search. The maximum deviation permitted for matching the peptide mass values was set at 100 ppm. Scores of  $>71$  were considered significant ( $p < 0.005$ ).

## 2.7 Real-time quantitative analysis

After incubating for 6 and 12 h under normoxic or hypoxic conditions, total RNA was extracted from mycelia and applied (2.0  $\mu$ g) to first-strand cDNA synthesis as described [26]. Real-time quantitative PCR was performed using a MiniOpticon™ (BioRad). Gene-specific primers were designed based on the sequence data ([http://www.broad.mit.edu/annotation/genome/aspergillus\\_nidulans](http://www.broad.mit.edu/annotation/genome/aspergillus_nidulans)) of 17 genes so that the lengths of the PCR products ranged between 160 and 190 bp. Real-time PCR proceeded in a final volume of 50  $\mu$ L. The SYBR® *Premix Ex Taq*™ (BioRad) was applied according to the manufacturer's instructions at a final concentration of 0.2  $\mu$ M and then PCR proceeded as follows: (i) initial denaturation at 94°C for 1 min, (ii) 40 cycles of denaturation at 94°C for 10 s, annealing at 62°C at 30 s, and elongation at 72°C for 20 s. Specific amplification was confirmed by analyzing melting curves from 65 to 95°C. Fluorescence was undetectable in a control experiment without a template. Table 1 lists the primers used for real-time PCR.

## 2.8 LC-ESI-TOF-MS analysis

The mycelia were incubated under normoxic and hypoxic conditions for 12 h at 30°C then separated from the medium by filtration, washed five times with chilled water, and lyophilized. Freeze-dried mycelia (50 mg) were immediately transferred into liquid nitrogen, ground into a fine powder, and then suspended in 100  $\mu$ L of methanol/water (50:50 v/v). After incubating at room temperature for 16 h, the extract was centrifuged at 11 000  $\times g$  for 5 min at room temperature then the supernatant was transferred to 1.5 mL tubes.

Metabolites were identified using a LC-ESI-TOF MS system in positive and negative ionization modes. Samples were separated by HPLC using an ACQUITY UPLC (Waters, Milford, MA, USA) equipped with an ACQUITY UPLC HSS T3 of 2.1 mm  $\times$  50 mm (Waters) and then fractions (5  $\mu$ L) were eluted using Gradient LC with 0.1% formic acid in ACN as mobile phase A and 0.1% formic acid v/v in water as mobile phase B. The initial mobile phase comprised 2% A for 1.5 min, followed by a linear gradient to 100% A for 6.75 min. The flow rate was 0.4 mL/min. The HPLC system was connected to a TOF mass spectrometer (LCT Premier XE, Waters, MA, USA) operating under the following conditions: desolvation gas flow, 550 L/h; cone gas flow, 50 L/h; desolvation temperature, 350°C; source temperature, 100°C. Leucine enkephalin (1 ng/ $\mu$ L) was the reference. Spectra were acquired over the  $m/z$  50–1000 range at a scan rate of 0.05 s/spectrum. The entire mass spectra were processed using MassLynx software (Waters) and Metalys2 (Genaris, Tokyo).

## 2.9 Other methods

Ammonia, nitrate, and nitrite were determined as described [10–12]. Nitrite was extracted from *A. nidulans* cells by incubating broken cells (see Section 2.2) with ice cold water for

**Table 1.** Primers used for real-time PCR

Gene	Primer sequence <sup>a)</sup>	Gene	Primer sequence <sup>a)</sup>
AN0893.3	F; 5'-ACCTCACCAAGCTCGACATC-3' R; 5'-ATGGTGTGCTCTTCCAACC-3'	AN5939.3	F; 5'-ACACGACCACCTTCCTTGAC-3' R; 5'-GTCTTCCATATCGCCCAGAA-3'
AN1965.3	F; 5'-CAAACATCATGGCAAACATGC-3' R; 5'-AGATTCTCCCGATCCACTT-3'	AN6157.3	F; 5'-GAAAACCAACGTCACCGTCT-3' R; 5'-ACTTGCGGTCCTCAAAGATG-3'
AN2440.3	F; 5'-GCCAAATTTGTCGGTATTGG-3' R; 5'-GAATGGCATCGAAATCCACT-3'	AN6209.3	F; 5'-CAGCTCGTCACTGTTGAAA-3' R; 5'-CTTGTCGTGATCTCCGTTGA-3'
AN2448.3	F; 5'-CCATTCACTGAGGGTGGT-3' R; 5'-CCATATCGGGAGGAGTCTCA-3'	AN6490.3	F; 5'-TGTATGCCTTCGTTTGTGGA-3' R; 5'-GAACAGGTGAAAGCACAGCA-3'
AN2867.3	F; 5'-CTGCAACCTCTTCGACAACA-3' R; 5'-AGAACTCAGACTGGATCGAA-3'	AN6542.3	F; 5'-GAAGTCTACGAACTGCCTGATG-3' R; 5'-AAGAACGCTGGGCTGGAA-3'
AN4464.3	F; 5'-ATCGAAGAGGCTGTTGAGG-3' R; 5'-TCGTAGTCCGAGTGTGTTTC-3'	AN7141.3	F; 5'-GCGATCGGCTCTCTGAATAC-3' R; 5'-GACGGAGACCACCCTGAGTA-3'
AN5447.3	F; 5'-TCTCTAAGGGCGCTTCACAT-3' R; 5'-CGCTGGCTCATGATGATAAA-3'	AN7588.2	F; 5'-TATTCATGAGGAGGGGATGC-3' R; 5'-GAAGTCTGAGGCCATGAAC-3'
AN5884.3	F; 5'-GGAGCGGGTTAGTGAGAGTG-3' R; 5'-ATACCTCGCCGGTAATCTT-3'	AN10230.3	F; 5'-GGCGGCTCTGTGATTAACAT-3' R; 5'-TGACAAAGTGCTTTGCGTTC-3'

a) F, forward primer; R, reverse primer.

1 h. The protein concentration was determined using a BioRad protein assay kit (BioRad). The oxygen concentration and dry weight of mycelia were determined as described [10–12]. Total DNA of *A. nidulans* was prepared as described [12]. DNA bases in the total DNA were determined as described by Spencer *et al.* [23].

### 3 Results and discussion

#### 3.1 Hypoxic ammonia fermentation

We cultured *A. nidulans* A26 in the presence of 10 mM nitrate and 100 mM ethanol to confirm ammonia-fermenting activity. The fungus consumed nitrate under both normoxic and hypoxic conditions. The hypoxic culture under low O<sub>2</sub> tension (<2 μM) concomitantly produced ammonia throughout the incubation period, whereas the normoxic culture produced none (Fig. 1A). Nitrite was undetectable in the culture medium. These observations closely correlated with previous findings indicating that nitrate is reduced to ammonia, which is then excreted into the culture medium and critical for the growth of *A. nidulans* under hypoxic conditions [12, 13]. Here, we found that nitrite accumulated in the cells as the incubation proceeded (Fig. 1B). This phenomenon was specific to cells cultured under hypoxic conditions. As reported [12] *A. nidulans* grew more slowly and reduced less nitrate under hypoxic conditions (Figs. 1A, B). However, considering the fungal cell mass, more nitrate was consumed under hypoxic, than normoxic (3–5 vs. 1–3 mM/mg cell protein) conditions, findings that are consistent with hypoxic nitrate reduction to ammonia. The lower growth rates under hypoxic than normoxic conditions is consistent

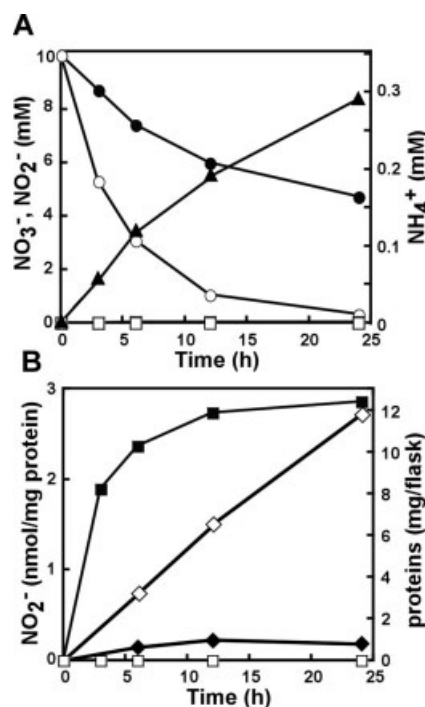


**Figure 1.** Nitrogen metabolism by *A. nidulans* A26 during normoxic and hypoxic culture. (A) *A. nidulans* A26 was cultured in medium containing 10 mM NaNO<sub>3</sub> (nitrogen source) under normoxic (open symbols) and hypoxic (closed symbols) conditions. Circles, nitrate; squares, nitrite; triangles, ammonium. (B) *A. nidulans* A26 cultured as in A under normoxic (open symbols) and hypoxic (closed symbols) conditions, and intracellular nitrite levels were determined. Total cellular proteins that increased during incubation are indicated as diamonds. Initial amount of total protein, 6.3 mg/flask. Experiments were repeated three times. SD of all data was <10%.

with the free energy change of  $-313$  kJ/mol for the oxidation of ethanol to acetate by nitrate, which is considerably lower than that for the oxidation of ethanol to carbon dioxide by dioxygen ( $-1324$  kJ/mol). Since, an electron acceptor is a critical factor that limits cell growth [12], slower reduction rates of nitrate under hypoxic conditions ( $8\text{--}17$   $\mu\text{M}/\text{h}$ , Fig. 1A) than dioxygen under normoxic conditions ( $\sim 200$   $\mu\text{M}/\text{h}$ , data not shown) also probably affected the growth rate. Upon incubation under hypoxic conditions for up to 24 h, the ratio of the fungal biomass (data not shown) and total cellular proteins (Fig. 1B) were constant ( $0.054 \pm 0.002$  g protein/g dry cell weight), indicating that the lack of dioxygen did not result in either autolysis or cell death during which intracellular proteins are released from the cells.

### 3.2 Comparative proteomic analysis

The 2-DE proceeded using IPG gels at  $pI$  4–7 (Figs. 2 and 3) and at  $pI$  6–11 (Figs. 2 and 4). We analyzed intracellular proteins in the fungus cultured for 6, 12, and 24 h under normoxic or hypoxic conditions. The experiments were repeated three times and the expression level of each respective protein spot was determined as average fluorescent intensity. Over 900 spots from cells cultured for 6, 12, and 24 h (Table 2) were visualized on the gels, and 322 spots (300 protein species) were identified *via* PMF analysis (Fig. S1 and Table S1 in Supporting Information). By comparing 2-DE gel profiles from different aeration conditions and culture stages (Figs. 2–4), we identified protein spots with intensity that was over double or less than half in one culture condition

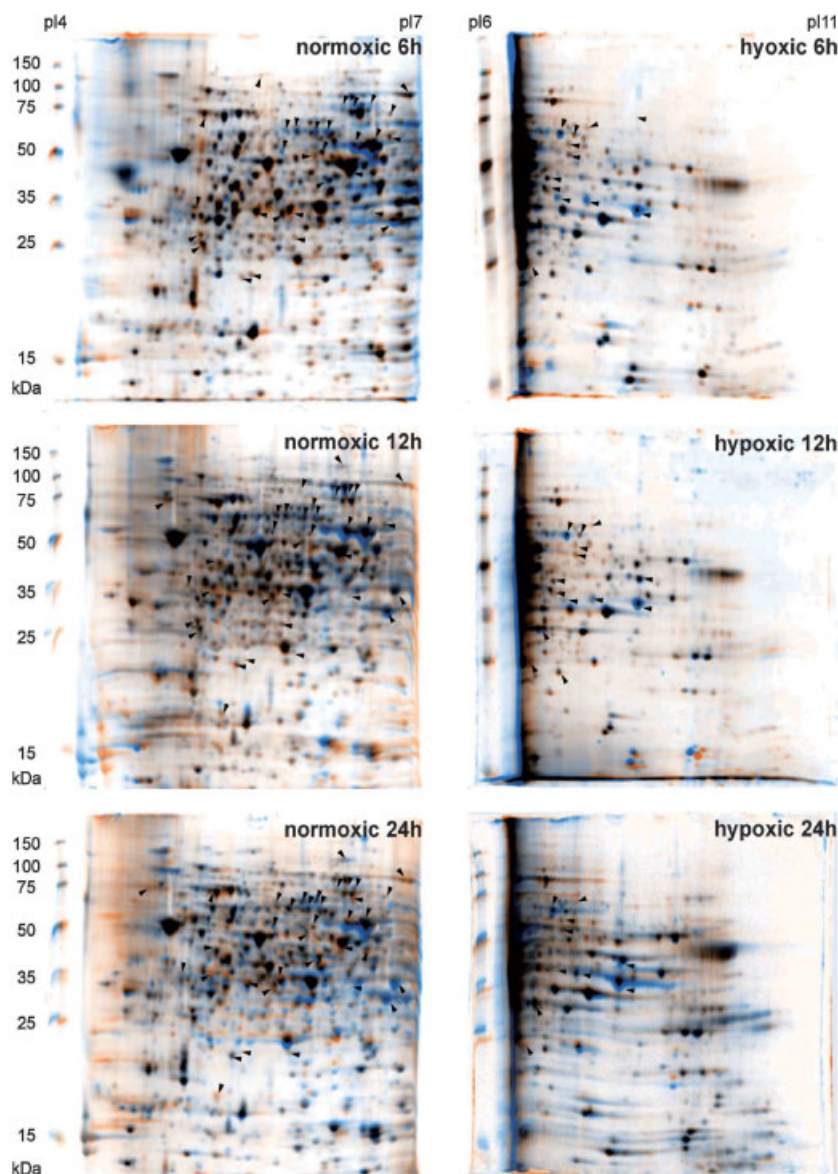


**Figure 2.** Time-dependent changes in proteome map of *A. nidulans* A26. Mycelia were incubated for 6, 12 and 24 h at 30°C under normoxic and hypoxic conditions. Intracellular proteins in lysed cells were separated by electrophoresis on IPG gels ( $pI$  4–7, left;  $pI$  6–11, right) and by SDS-PAGE, and images were overlaid with Proteome-weaver software. Spots detected in the normoxic and hypoxic samples are shown in blue and orange, respectively. Overlap of spots from both gels is shown in black. Arrowheads indicate spots of which volumes changed over time.

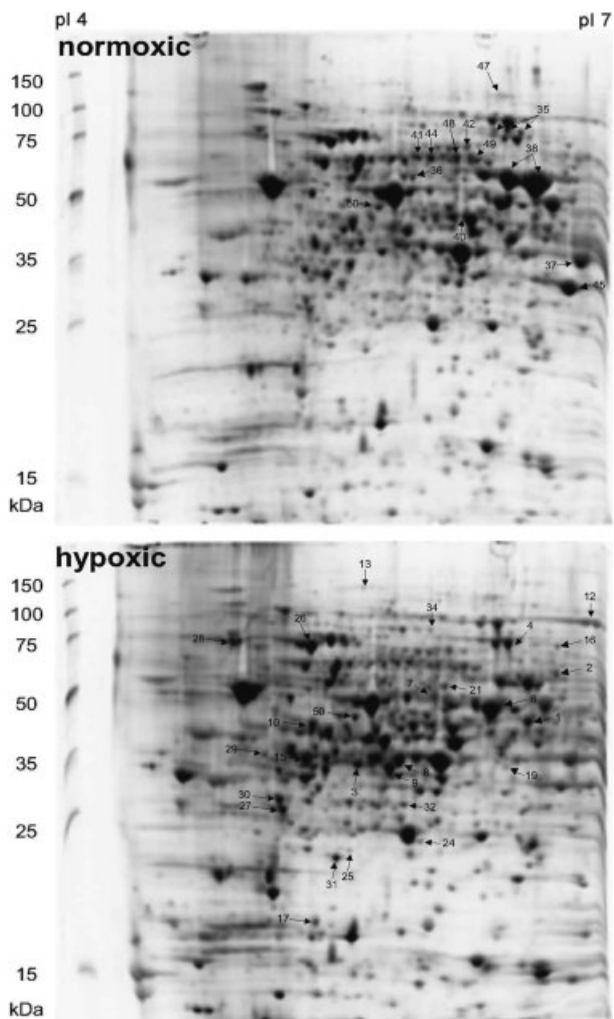


**Figure 3.** Proteome map of *A. nidulans* A26. Mycelia were incubated for 12 h at 30°C under normoxic (upper panel) and hypoxic (lower panel) conditions. Intracellular proteins in lysed cells were separated by electrophoresis on IPG gels (pI 4–7) and by SDS-PAGE. Identified protein spots are marked by arrows with numbers (Table 3).

compared with the other and designated the corresponding proteins as up- or downregulated. The results showed that 63 and 41 proteins were up- and downregulated, respectively under hypoxic conditions, while the expression level of actin (*actA* gene product) (spot 50, Fig. 3, Table 3) remained constant. Among them, PMF analysis identified 49 proteins (Figs. 3 and 4). Table 3 summarizes the quantitative findings for these proteins.

### 3.3 Glycolysis, gluconeogenesis, TCA and glyoxylate (GLOX) cycles, and glutamate metabolism

Among the glycolytic enzymes, pyruvate dehydrogenase was induced under hypoxic conditions while the expression of fructose-1, 6-bisphosphate aldolase, triose-phosphate isom-

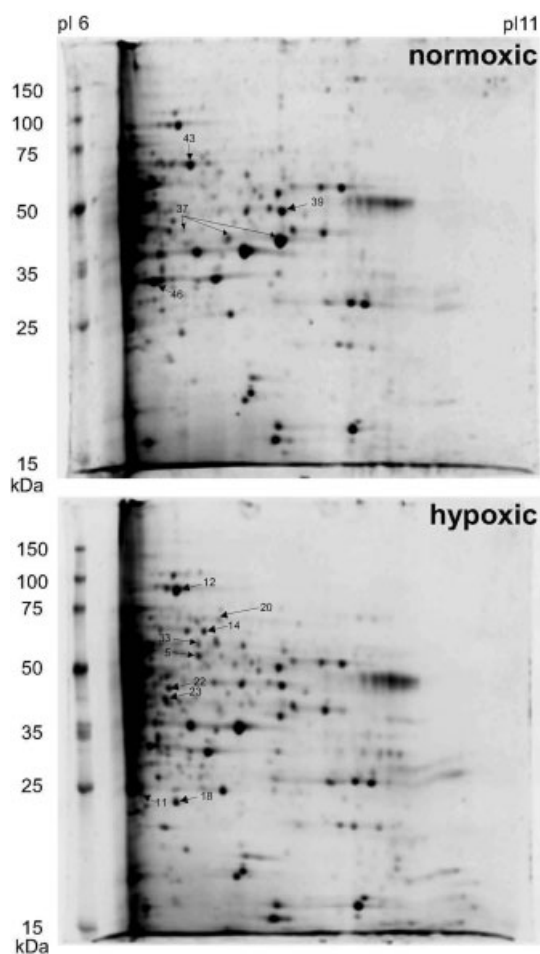


**Figure 4.** Proteome map of *A. nidulans* A26. Mycelia were incubated for 12 h at 30°C under normoxic (upper panel) and hypoxic (lower panel) conditions. Intracellular proteins in lysed cells were separated by electrophoresis on IPG gels (pI 6–11) and by SDS-PAGE. Identified protein spots are marked by arrows with numbers (Table 3).

erase, glyceraldehyde-3-phosphate dehydrogenase, enolase, and phosphoglycerate kinase remained constant (Figs. 2–4, Table 3). Phosphoenolpyruvate carboxykinase and malic enzyme, which are involved in gluconeogenesis, were repressed compared with those under normoxic conditions. The amount of intracellular glucose was 2.1-fold less under hypoxic conditions (data not shown), indicating that cells were more starved for glucose when cultured under hypoxia than under normoxia. The production of typical proteins in the TCA cycle was also dependent upon aeration. Isocitrate dehydrogenase, aconitase, and succinate dehydrogenase levels remained constant at 6, 12, and 24 h under hypoxic conditions, while citrate synthase, 2-oxoglutarate dehydrogenase, and malate dehydrogenase were downregulated (Figs. 2–4, Table 3). Levels of fumarate reductase, NADH-ubiquinone oxidoreductase, and ATP synthase remained constant irrespective of aeration (Figs. 2–4, Table 3).

**Table 2.** Summary of *A. nidulans* proteins identified by 2-DE

	pI 4–7				pI 6–11			
	No. of detected protein spots		No. of upregulated proteins		No. of detected protein spots		No. of upregulated proteins	
	N	H	N	H	N	H	N	H
6 h	603	606	31	38	225	231	13	22
12 h	655	659	32	48	253	260	19	27
24 h	644	650	35	42	214	218	17	24

*A. nidulans* A26 was cultured under normoxic (N) and hypoxic (H) conditions. Proteins were designated as upregulated when intensity of corresponding spots was greater than double or less than half that in gel showing other culture condition.

Isocitrate lyase functioning in the GLOX cycle was significantly downregulated, indicating decreased metabolic flow to GLOX cycle under hypoxic conditions. These findings are consistent with the fact that no glyoxisome (peroxisome) is generated by *S. cerevisiae* under anaerobic conditions [24] and indicated that the flux of the central metabolic pathway was obviously changed under hypoxic conditions.

We showed that NADP<sup>+</sup>-dependent glutamate dehydrogenase (NADP-GDH) encoded by the *gdhA* gene is upregulated under hypoxic conditions (Figs. 2 and 3 and Table 3). NADP-GDH is versatile in fungi and functions in ammonia assimilation by synthesizing glutamate through the reductive amination of 2-oxoglutarate [25, 26]. A role of NADP-GDH in detoxifying ammonia has also been reported [27, 28]. The induction of NADP-GDH in hypoxic cells suggests that the fungus assimilates and/or detoxifies ammonia under these culture conditions. The production of NADP-GDH is induced by ammonia at the transcriptional level [29, 30]. We showed that when cultured under hypoxic conditions, the cells accumulated ammonia (Fig. 1A), which induces *gdhA* expression.

Under hypoxic conditions,  $\gamma$ -aminobutyrate (GABA) transaminase and a putative succinic semialdehyde dehydrogenase were upregulated by incubating for 12 and 24 h under hypoxic conditions (Figs. 2–4, Table 2). Reports have shown that GABA is generated from 2-oxoglutarate *via* glutamate through the actions of glutamate dehydrogenase and glutamate decarboxylase, and that GABA transaminase irreversibly transaminates GABA to succinic semialdehyde, which is then oxidized to succinate by succinic semialdehyde dehydrogenase. This reaction is physiologically significant as it bypasses the TCA cycle and is referred to the GABA shunt [31, 32]. We detected expression of the genes for GABA transaminase (AN2248.3) and the putative succinic semialdehyde dehydrogenase (AN7141.3) was upregulated in the hypoxic cells (Table 4) as well as the corresponding proteins (Table 3). The gene for glutamate decarboxylase (AN5447.3) was upregulated under hypoxic conditions (Table 4), indicating that the GABA shunt is more active under such circumstances. The increase of glutamate dehydrogenase (Table 3)

that supplies glutamate for the GABA shunt also supports this notion. The physiological significance of the GABA shunt in the absence of O<sub>2</sub> remains obscure, but it might function in regulating the NADH/NAD<sup>+</sup> balance in the cells. Although nitrate serves as electron acceptor under hypoxic conditions, this function is insufficient to re-oxidize NADH–NAD<sup>+</sup>, and would result in a high NADH/NAD<sup>+</sup> ratio. In the GABA shunt, NADH-GDH oxidizes NAD(P)H and succinic semialdehyde dehydrogenase reduces NAD(P)<sup>+</sup> to generate NAD(P)H and thus no NAD(P)<sup>+</sup> is produced *via* this pathway. This is in contrast to the oxidative conversion of 2-oxoglutarate to succinate in the conventional TCA cycle, in which 2-oxoglutarate dehydrogenase, and succinyl CoA synthetase perform the catalysis, generating one molecule of NADH *per* conversion of one 2-oxoglutarate molecule to succinate. Under hypoxic conditions, 2-oxoglutarate dehydrogenase was downregulated (Table 3) and a high NADH/NAD<sup>+</sup> ratio led to the inactivation of 2-oxoglutarate dehydrogenase, indicating that the metabolic flow from 2-oxoglutarate to glutamate is more activated than under normoxic conditions. The similar activation of the GABA shunt in *F. oxysporum* cultured under anoxic conditions [32, 33], suggests a popular role of the shunt in hypoxia.

### 3.4 Pentose and nucleotide metabolisms under hypoxic conditions

We found that glucose-6-phosphate dehydrogenase (G6PDH), transaldolase, and transketolase typical proteins constituting the pentose-phosphate pathway (PPP), were upregulated under hypoxic conditions (Figs. 2 and 3, Table 3). One of the physiological functions of PPP is the generation of NADPH, which might serve as a substrate for NADPH dehydrogenases including NADP-GDH, succinic semialdehyde dehydrogenase, sulfite reductase, nitroreductase, and quinone reductase, which were induced under hypoxic conditions (Table 3). We also found that enzymes involved in nucleotide metabolism such as bifunctional purine biosynthesis protein (*purH*) (AN4464.3), orotate phosphoribosyltransferase (AN5884.3), and purine nucleotide

**Table 3.** Identified proteins of *A. nidulans* cultured under normoxic and hypoxic conditions

No.	Annotation name		6 h <sup>a)</sup>	12 h <sup>a)</sup>	24 h <sup>a)</sup>	Score	tpI <sup>b)</sup>	tMW <sup>c)</sup>	MP <sup>d)</sup>	Cov. <sup>e)</sup>
<b>Upregulated proteins under hypoxic conditions</b>										
Glycolysis										
1	Pyruvate dehydrogenase E1 component subunit alpha	AN5162.3 <sup>f)</sup>	1.8	2.5	2.6	94	8.18	45.5	9/13	24
PPP										
2	Glucose-6-phosphate dehydrogenase	AN2981.3	2.9	2.0	1.7	164	6.27	59.0	15/17	41
3	Transaldolase	AN0240.3	3.3	1.5	2.4	135	5.31	35.5	11/13	31
4	Transketolase	AN0688.3	1.5	1.1	4.8	192	5.85	75.5	23/29	41
GABA shunt										
5	GABA aminotransferase	AN2248.3	3.3	5.7	2.2	120	8.92	55.5	14/23	27
6	Glutamate dehydrogenase	AN4376.3	2.2	2.9	3.4	159	6.07	49.6	15/24	47
7	Succinic-semialdehyde dehydrogenase	AN7143.3	3.6	1.8	2.2	71	5.76	51.3	7/12	22
Thiamine synthesis										
8	Pyrimidine biosynthetic enzyme (THI5)	AN8009.3	5.0	2.8	3.0	155	5.74	38.2	12/14	44
9	Thiazole biosynthetic enzyme (THI4)	AN3928.3	8.1	7.6	14.2	131	5.48	35.6	15/24	43
Sulfur metabolism										
10	S-Adenosylmethionine synthase	AN1222.3	1.1	3.5	2.8	198	5.30	42.2	17/24	52
11	Adenylylsulfate kinase	AN1194.3	unique	unique	unique	80	6.60	23.0	6/9	36
12	Methionine synthase	AN4443.3	2.9	2.5	5.0	122	6.36	86.8	14/17	24
13	Putative sulfite reductase	AN1752.3	2.8	1.3	1.8	71	5.00	114.8	8/14	15
14	Sulfate adenylyltransferase	AN4769.3	4.1	2.4	1.8	192	6.87	63.9	22/28	44
Nucleotide metabolism										
15	Adenosine kinase	AN2272.3	2.5	1.6	3.0	120	5.31	38.3	11/18	38
16	Bifunctional purine biosynthesis protein (PurH)	AN4464.3	2.2	1.4	3.0	105	6.31	65.6	12/16	31
17	dUTPase	AN0271.3	0.7	3.4	3.6	109	6.15	21.5	7/12	43
18	Orotate phosphoribosyltransferase	AN5884.3	1.8	2.7	1.6	72	6.85	25.4	5/7	27
19	Phosphorylase	AN10230.3	unique	2.9	unique	93	6.62	39.5	7/11	30
Fatty acid metabolism										
20	ATP-citrate lyase subunit A	AN2436.3	unique	unique	unique	92	8.20	71.5	8/10	18
21	ATP-citrate lyase subunit B	AN2435.3	3.2	2.6	3.7	213	5.80	53.0	21/26	41
22	Acetoacetyl-CoA thiolase	AN1409.3	2.4	2.0	1.8	82	7.04	42.0	7/10	27
Others										
23	ADH	AN8979.3	2.4	2.2	1.8	103	7.59	37.1	9/19	43
24	Carbonic anhydrase family protein	AN1805.3	1.2	2.4	unique	75	5.8	24.8	6/8	22
25	Elongation factor 1B	AN9304.3	2.6	2.6	3.0	74	5.36	24.0	4/7	28
26	Heat-shock protein 70	AN10202.3	3.8	1.4	2.9	179	5.24	67.0	18/25	38
27	Inorganic phosphatase	AN2968.3	2.7	2.4	1.9	93	5.36	33.9	10/13	30
28	78 kDa glucose-related protein	AN2062.3	1.9	3.0	2.5	238	4.84	73.7	26/29	45
29	Methyltransferase	AN9098.3	2.7	2.0	unique	70	5.38	29.9	5/8	30
30	NADH-ubiquinone reductase subunit	AN5971.3	3.4	2.1	2.6	74	5.09	27.1	6/9	24
31	Nitroreductase	AN2343.3	2.2	4.1	2.0	94	5.45	24.5	6/7	31
32	Quinone reductase	AN7914.3	2.2	2.0	1.2	62	4.99	36.0	5/7	27
33	Septin B	AN6688.3	2.7	4.2	2.2	85	6.70	46.8	9/11	25
34	Tryptophan synthase	AN6231.3	1.7	2.5	1.6	69	5.75	77.5	7/12	15
<b>Downregulated proteins under hypoxic conditions</b>										
35	ACS	AN5626.3	0.21	0.34	0.40	161	6.0	74.3	19/23	31
36	Alanine aminotransferase	AN1923.3	0.28	0.41	0.48	155	5.6	54.8	12/16	37
37	ADH	AN8979.3	0.16	0.19	0.21	93	7.6	37.1	8/19	38
38	ALDH	AN0554.3	0.19	0.12	0.18	249	6.2	54.2	25/32	43
39	Citrate synthase	AN8275.3	0.80	0.41	0.31	77	8.7	52.2	8/12	26
40	Flavohemoglobin	AN7169.3	0.48	0.60	0.41	79	6.0	44.9	8/11	25
41	GMC oxidoreductase	AN7267.3	0.35	0.45	0.78	72	5.7	59.2	6/10	19

**Table 3.** Continued

No.	Annotation name		6 h <sup>a)</sup>	12 h <sup>a)</sup>	24 h <sup>a)</sup>	Score	tp <sup>b)</sup>	tMW <sup>c)</sup>	MP <sup>d)</sup>	Cov. <sup>e)</sup>
42	GMC oxidoreductase	AN8547.3	0.68	0.88	0.43	74	5.6	64.5	7/12	22
43	Isocitrate lyase	AN5634.3	0.23	0.21	0.22	171	6.5	60.2	14/17	43
44	Malic enzyme	AN6168.3	0.18	0.47	0.36	86	6.6	71.8	16/21	27
45	Malate dehydrogenase	AN6499.3	0.35	0.31	0.14	110	5.8	33.3	11/15	39
46	Malate dehydrogenase	AN6717.3	0.72	0.40	0.89	124	6.9	37.7	10/13	41
47	2-Oxoglutarate dehydrogenase	AN5571.3	0.59	0.50	0.48	90	6.4	117.9	12/16	18
48	Phosphoenolpyruvate carboxykinase	AN1918.3	0.22	0.40	0.45	139	5.8	61.4	11/16	29
49	UTP-glucose-1-phosphate uridylyltransferase	AN9094.3	0.36	0.65	0.92	89	6.0	55.8	8/15	24
<b>Constantly-produced proteins</b>										
50	Actin	AN6542.3	1.3	1.1	1.0	135	5.5	41.7	13/17	38

a) Levels of expression compared under hypoxic and normoxic conditions. SDs of each data were less than 31%.  $p < 0.05$ .

b) Theoretical  $pI$ .

c) Theoretical mass.

d) Numbers of peptides of which mass matched theoretical numbers of peptides.

e) Sequence coverage (%) in PMF.

f) Protein names and accession numbers are according to the *A. nidulans* genome database: [http://www.broad.mit.edu/annotation/genome/aspergillus\\_nidulans/MultiHome.html](http://www.broad.mit.edu/annotation/genome/aspergillus_nidulans/MultiHome.html).

**Table 4.** Expression of genes for glutamate, pentose, and nucleotide metabolism

Annotation name	Gene name	Fold change <sup>a)</sup>	
		6 h	12 h
<b>GABA shunt</b>			
Glutamate decarboxylase	AN5447.3	4.1	5.6
GABA transaminase	AN2248.3 <sup>b)</sup>	3.1	7.5
Putative succinic semialdehyde dehydrogenase	AN7141.3 <sup>b)</sup>	2.6	2.1
<b>PPP</b>			
Ribose-phosphate pyrophosphokinase	AN1965.3	1.5	3.7
Ribose 5-phosphate isomerase	AN2440.3	1.8	4.0
Phosphoglucomutase	AN2867.3	3.9	5.2
Ribulose-phosphate 3-epimerase	AN7588.3	4.1	6.5
<b>Nucleotide synthesis</b>			
Orotate phosphoribosyltransferase	AN5884.3 <sup>b)</sup>	2.9	7.6
Orotidine-phosphate decarboxylase	AN6157.3	2.9	5.4
Bifunctional purine biosynthesis protein (PurH)	AN4464.3 <sup>b)</sup>	2.2	4.1
Adenosylsuccinate synthase	AN0893.3	1.0	3.1
Adenosylsuccinate lyase	AN6209.3	2.1	3.3
<b>Nucleotide degradation</b>			
5'-Nucleotidase	AN5939.3	3.0	3.8
Purine nucleotide phosphorylase	AN6490.3	2.4	3.4
Purine nucleotide phosphorylase	AN10230.3 <sup>b)</sup>	2.5	2.9

Transcripts quantified by real-time PCR by using total RNA prepared from *A. nidulans* grown under normoxic and hypoxic conditions. Data are shown as relative expression rates and are normalized to  $\beta$ -actin (*actA*) transcript. Experiments were repeated three times. SD of all data was  $< 10\%$ .

a) Fold changes for cells cultured under hypoxic *versus* normoxic conditions.

b) Corresponding proteins identified on 2-DE.

phosphorylase (AN10230.3) were also upregulated under hypoxic conditions (Table 3). To further characterize the enzymes involved in these metabolic mechanisms, we used real-time PCR to measure the expression of 12 putative genes, nine of which were not identified in 2-DE gels (Table 4). The results showed that transcription of ribose-5-phosphate isomerase (AN2440.3), ribose-phosphate pyrophosphokinase (AN1965.3), orotate phosphoribosyltransferase (AN5884.3), and orotidine phosphate carboxylase (AN6157.3), which were involved in *de novo* synthesis of pyrimidine nucleotides (Fig. 5), and bifunctional purine biosynthesis protein (purH) (AN4464.3) involved in purine biosynthesis were activated, suggesting that metabolic flow from PPP to nucleotides is activated under hypoxic conditions. Furthermore, we found that the genes for degrading nucleotides, namely 5'-nucleotidase (AN5939.3), and purine nucleotide phosphorylase (AN10230.3 and AN6490.3) were also upregulated under hypoxic conditions. These enzymes digest both pyrimidine and purine nucleotides to generate nucleobases and ribose-1-phosphate (Fig. 5), the latter of which returns to enter PPP. These results imply that hypoxia activates the turnover of intracellular nucleotides and ribose phosphates. Intracellular nucleotides were analyzed using LC-ESI-TOF-MS. The observed molecular mass values were searched in the database (Chemical Entities of Biological Interest, EMBL-EBI) and identified. The results showed that more xanthosine ( $C_{10}H_{12}N_4O_6$ , observed  $m/z = 284.077009$ ,  $5.5 \times$ ), dTMP ( $C_{10}H_{15}N_2O_8P$ ,  $m/z = 322.058289$ ,  $2.8 \times$ ), deoxyadenosine ( $C_{10}H_{13}N_5O_3$ ,  $m/z = 251.101611$ ,  $2.5 \times$ ), adenine ( $C_5H_5N_5$ ,  $m/z = 135.055072$ ,  $2.2 \times$ ), thymidine ( $C_{10}H_{14}N_2O_5$ ,  $m/z = 242.090614$ ,  $2.1 \times$ ), and dAMP ( $C_{10}H_{14}N_5O_6P$ ,  $m/z = 331.069261$ ,  $2.0 \times$ ) were produced by *A. nidulans* grown under hypoxic, compared with normoxic conditions (molecular mass values and induction ratios are shown in parentheses). This indicated that ribose production was altered under hypoxic conditions, and supports the notion that nucleotide turnover is more active under hypoxic conditions.

Although little is known about organisms that anoxically activate nucleotide mechanisms,  $>100 \mu M$  nitrite leads to the deamination of purine bases in DNA from human epithelial cells [23]. Here, we found nitrite accumulation in hypoxic *A. nidulans* cells (Fig. 1B). We also found that DNA in the hypoxic cells contained 1.7- and 2.4-fold more xanthine and hypoxanthine, deaminated products of guanine and adenine than those in the normoxic cells (Table 5), which suggested that DNA became intracellularly damaged by nitrite. Damaged nucleotides must be enzymatically broken down through the activity of 5'-nucleotidase and purine nucleotide phosphorylase (which we found were upregulated under hypoxic conditions) and the resultant ribose phosphate moieties were recycled for nucleotide synthesis. Meanwhile, the successive reactions of adenosylsuccinate synthase and adenosylsuccinate lyase present another route for repairing deaminated purines (AMP) and for generating AMP from IMP, a deamination product of AMP *via* nitrite

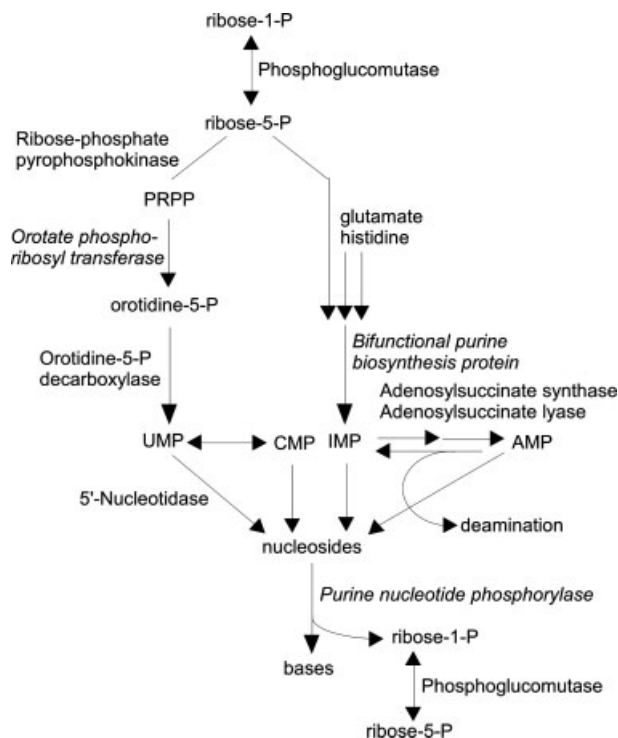


**Figure 5.** Schematic illustration of putative purine and pyrimidine metabolism in *A. nidulans* A26 under hypoxic conditions. Enzymes identified in 2-DE gels are shown in italics. Gene names for each enzyme are listed in Table 4. Orotidine-5-P, orotidine-5-phosphate; PRPP; ribose-1-P, D-ribose-1-phosphate; ribose-5-P, D-ribose-5-phosphate.

(Fig. 5). Real-time PCR analyses showed increased expression of the genes for these enzymes (AN0893.3 and AN6209.3) in the hypoxic cells (Table 4), indicating that the repair mechanism of purine nucleotides is more important for adapting to hypoxia. The upregulation of two HSPs (AN10102.3 and AN2062.3) was consistent with the notion that nitrite damaged the cells.

### 3.5 Thiamine biosynthesis

The production of thiazole biosynthetic protein (THI4) and pyrimidine biosynthetic protein (THI5), both of which play key roles in thiamine biosynthesis [34–36], was obviously increased (3.0- to 14.2-fold, respectively) under hypoxic conditions (Figs. 2 and 3, Table 3). These findings indicated that the biosynthesis of thiamine is more important under such conditions. Thiamine is converted to thiamine pyrophosphate (TPP), which is an essential coenzyme for the critical enzymes used in energy conservation [37, 38]. Such enzymes include transketolase in PPP and pyruvate dehydrogenase in glycolysis and levels of these were increased as above. This supports our claim that PPP and pentose/nucleotide synthesis are more active under hypoxic conditions. In *S. cerevisiae* and other eukaryotes, only the genes for thiamine biosyn-

**Table 5.** DNA base modification in *A. nidulans* under hypoxic conditions

Culture conditions	Amounts of bases (nmol/mg DNA)							
	Adenine	Cytosine	Guanine	Thymine	Hypoxanthine	Xanthine	8-OH-A	8-OH-G
Normoxic	120	116	130	113	0.55	0.98	0.022	0.020
Hypoxic	125	118	136	116	1.33	1.58	0.025	0.020

DNA prepared from *A. nidulans* cells was treated with formic acid and liberated bases were analyzed GC/MS as described in [13]. 8-OH-A, 8-hydroxy adenine; 8-OH-G, 8-hydroxy guanine. Experiments were repeated three times. SD of all data was <19%.

thesis identified so far are required for 4-methyl-5-( $\beta$ -hydroxyethyl) thiazole phosphate (thiazole moiety) (*THI4*) and 2-methyl-4-amino-5-hydroxymethylpyrimidine pyrophosphate (pyrimidine moiety) (*THI5*) biosynthesis. The postulated substrates for Thi4p are glycine, cysteine, and an unidentified precursor with five carbon (C5) atoms. The C5 precursor might originate from D-ribulose-5-phosphate or D-xylulose-5-phosphate, both of which are intermediates of the PPP [34, 35]. The pyrimidine moiety is synthesized by Thi5p from histidine and pyridoxine, the latter of which is also derived from 5-phosphoribosyl diphosphate (PRPP) produced *via* the PPP [34, 36]. The upregulation of Thi4 and Thi5 is hence consistent with PPP activation, which could supply C5 precursors for thiamine synthesis, and implies that one roles of PPP under hypoxic conditions is to supply more pentose-derived C5 compounds for thiamine synthesis.

### 3.6 Other proteins

Under hypoxic conditions, the expression level of alcohol dehydrogenase I (ADH) and ALDH, which play key roles in oxidating ethanol [12], was basal, in contrast to being obviously induced under normoxic conditions (Table 2). We have shown that the transcription factor AlcR induces expression of the genes for ADH (AN8979.3, *alcA*) and ALDH (AN0554.3, *aldA*) under hypoxic [12] as well as under normoxic [39] conditions. These results indicated that the activity of AlcR is differently regulated according to aerating conditions.

We reported that *A. nidulans* oxidizes ethanol to acetate through the activities of ADH, CoA-acylating ALDH, and Ack under hypoxic conditions. Among them ADH (as above) and Ack (FacA, AN5626.3, spot 35) were detected in the 2-DE gels. Ack gave three spots with slightly different molecular masses and pI. This is consistent with our previous observation that *A. nidulans* produced Ack isozymes with and without acetylated lysine residues [12]. Neither CoA-acylating ALDH nor ammonia producing enzymes (the *niaD* and *niiA* gene products) was detected in 2-DE gels. Hypoxia upregulates heme- and sterol-biosynthesis pathways in yeasts [7–9]. We did not identify any upregulated enzymes for these

pathways in our proteomes, probably because of low production levels. This is consistent with proteomes of other filamentous fungi [17].

We used sulfate as a sulfur source for *A. nidulans*. Sulfate adenyltransferase that catalyzes the initial step of sulfate assimilation was upregulated in hypoxic cells. This enzyme activates sulfate to phosphoadenosine 5-phosphosulfate (PAPS), and hence the increased production of sulfate adenyltransferase probably increased the PAPS level, which would have further increased the amount of enzyme substrate (PAPS) available for sulfate assimilation (NAD(P)H-, sulfate-, and sulfite-reductases). This consequently re-oxidizes the NAD(P)H that accumulates in hypoxic cells due to the lack of electron acceptors and supports cell growth under hypoxic conditions. Another reason for a higher rate of sulfate assimilation under hypoxic conditions might be an increased Cys requirement due to the unfavorable nitrosation of sulfhydryl Cys groups caused by hypoxic nitrite accumulation (Fig. 1B).

## 4 Concluding remarks

We applied a comparative proteomic approach to investigate hypoxia-induced responses by the model filamentous fungus *A. nidulans* and found that a series of enzymes involved in energy conservation, as well as carbohydrate, lipid, and sulfur metabolism were up- and downregulated. The metabolism of pentose and nucleotide metabolism was notably activated under hypoxia. The physiological relevance of this remains to be determined, but one explanation might be the synthesis of TPP cofactor for various metabolic enzymes. The upregulation of the enzymes for thiamine biosynthesis as well as TPP enzymes such as transketolase in PPP and pyruvate dehydrogenase supports this notion. The activation of nucleotide metabolism is of biological significance in that it increases nucleotide turnover to allow the degradation of damaged (deaminated) nucleotides and re-constructing nucleotides as discussed above. Another possible role of the upregulated nucleotide metabolism is the use of intracellular nucleoside pools as energy sources like human astrocytoma cells. Under ischemic conditions these cells are limited by the amount of energy available due to deficient respiration

and so they use nucleosides as an energy source [40]. In either or both circumstances, we consider that the activation of nucleotide salvage is a fungal mechanism of adaptation to hypoxia. We have shown that *A. nidulans* expresses nitrate reduction mechanisms for utilizing nitrate as an electron acceptor under hypoxic conditions, and this is considered a mechanism of adaptation to hypoxia [12]. Both mechanisms constitute a fungal strategy for survival under hypoxic conditions.

We thank Dr. T. Baba (University Tsukuba) for help with the gel-imaging and Norma Foster for critical reading the paper. This study was partly supported by the Bio-oriented Technology Research Advancement Institution, the COE program of University of Tsukuba, and a Grant-in-Aid for Scientific Research from the Ministry of Education, Science, Culture and Sports, Japan.

The authors have declared no conflict of interest.

## 5 References

- [1] Rocha, S., Gene regulation under low oxygen: holding your breath for transcription. *Trends Biochem. Sci.* 2007, **32**, 389–397.
- [2] ter Linde, J. J. M., Liang, H., Davis, R. W., Steensma, H. Y. *et al.*, Genome-wide transcriptional analysis of aerobic and anaerobic chemostat cultures of *Saccharomyces cerevisiae*. *J. Bacteriol.* 1999, **181**, 7409–7413.
- [3] Piper, M. D. W., Daran-Lapujade, P., Bro, C., Regenber, B. *et al.*, Reproducibility of oligonucleotide microarray transcriptome analyses. An interlaboratory comparison using chemostat cultures of *Saccharomyces cerevisiae*. *J. Biol. Chem.* 2002, **277**, 37001–37008.
- [4] Kwast, K. E., Lai, L., Menda, N., James, D. T. *et al.*, Genomic analyses of anaerobically induced genes in *Saccharomyces cerevisiae*: Functional roles of Rox1 and other factors in mediating the anoxic response. *J. Bacteriol.* 2002, **184**, 250–265.
- [5] Kobi, D., Zugmeyer, S., Potier, S., Jaquet-Gutfreund, L., Two-dimensional protein map of an "ale"-brewing yeast strain: proteome dynamics during fermentation. *FEMS Yeast Res.* 2004, **5**, 23–230.
- [6] de Groot, M. J. L., Daran-Lapujade, P., van Breuklen, B., Knijnenburg, T. A. *et al.*, Quantitative proteomics and transcriptomics of anaerobic and aerobic yeast cultures reveals post-transcriptional regulation of key cellular processes. *Microbiology* 2007, **153**, 3864–3878.
- [7] Keng, T., *HAP1* and *ROX1* form a regulatory pathway in the repression of *HEM13* transcription in *Saccharomyces cerevisiae*. *Mol. Cell. Biol.* 1992, **12**, 616–2623.
- [8] Zitomer, R. S., Lowry, C. V., Regulation of gene expression by oxygen in *Saccharomyces cerevisiae*. *Microbiol. Rev.* 1992, **56**, 1–11.
- [9] Todd, B. L., Stewart, E. V., Burg, J. S., Hughes, A. L., Espen-shade, P. J., Sterol regulatory element binding protein is a principal regulator of anaerobic gene expression in fission yeast. *Mol. Cell. Biol.* 2006, **26**, 2817–2831.
- [10] Zhou, Z., Takaya, N., Sakairi, M. A. C., Shoun, H., Oxygen requirement for the denitrification by the filamentous fungus *Fusarium oxysporum*. *Arch. Microbiol.* 2001, **175**, 19–25.
- [11] Zhou, Z., Takaya, N., Nakamura, A., Yamaguchi, M. *et al.*, Ammonia fermentation, a novel anoxic metabolism of nitrate by fungi. *J. Biol. Chem.* 2002, **277**, 1892–1896.
- [12] Takasaki, K., Shoun, H., Yamaguchi, M., Takeo, K. *et al.*, Fungal ammonia fermentation-A novel metabolic mechanism that couples the dissimilatory and assimilatory pathways of both nitrate and ethanol. *J. Biol. Chem.* 2004, **279**, 12414–12420.
- [13] Takasaki, K., Shoun, H., Nakamura, A., Hoshino, T., Takaya, N., Unusual transcription regulation of the *niaD* gene under anaerobic conditions supporting fungal ammonia fermentation. *Biosci. Biotechnol. Biochem.* 2004, **68**, 978–980.
- [14] Kim, Y., Nandakumar, M. P., Marten, M. R., Proteomics of filamentous fungi. *Trends Biotechnol.* 2007, **25**, 395–400.
- [15] Carberry, S., Neville, C. M., Kavanagh, K. A., Doyle, S., Analysis of major intracellular proteins of *Aspergillus fumigatus* by MALDI mass spectrometry: Identification and characterisation of an elongation factor 1B protein with glutathione transferase activity. *Biochem. Biophys. Res. Commun.* 2006, **341**, 1096–1104.
- [16] Fernandez-Acero, F. J., Jorge, I., Calvo, E., Vallejo, I. *et al.*, Two-dimensional electrophoresis protein profile of the phytopathogenic fungus *Botrytis cinerea*. *Proteomics* 2006, **6**, 88–96.
- [17] Shimizu, M., Yuda, N., Nakamura, T., Tanaka, H. *et al.*, Metabolic regulation at the tricarboxylic acid and glyoxylate cycles of the lignin-degrading basidiomycete *Phanerochaete chrysosporium* against exogenous addition of vanillin. *Proteomics* 2005, **5**, 3919–3931.
- [18] Grinyer, J., McKay, M., Nevalainen, H., Herbert, B. R., Fungal proteomics: Mapping the mitochondrial proteins of a *Trichoderma harzianum* stain applied for biological control. *Curr. Genet.* 2005, **45**, 237–247.
- [19] Kim, Y., Nandakumar, M. P., Marten, M. R., Proteome map of *Aspergillus nidulans* during osmoadaptation. *Fungal Genet. Biol.* 2007, **44**, 886–895.
- [20] Melin, P., Schnurer, J., Wagner, E. G. H., Proteome analysis of *Aspergillus nidulans* reveals proteins associated with the response to the antibiotic concanamycin A, produced by *Streptomyces* species. *Mol. Genet. Genomics* 2002, **267**, 695–702.
- [21] Hortschansky, P., Eisendle, M., Al-Abdallah, Q., Schmidt, A. D. *et al.*, Interaction of HapX with the CCAAT-binding complex-a novel mechanism of gene regulation by iron. *EMBO J.* 2007, **26**, 3157–3168.
- [22] Challapalli, K. K., Zabel, C., Schuchhardt, J., Kaindl, A. M. *et al.*, High reproducibility of large-gel two-dimensional electrophoresis. *Electrophoresis* 2004, **25**, 3040–3047.
- [23] Spencer, J. P., Whiteman, M., Jenner, A., Halliwell, B., Nitrite-induced deamination and hypochlorite-induced oxidation of DNA in intact human respiratory tract epithelial cells. *Free Radic. Biol. Med.* 2000, **28**, 1039–1050.
- [24] Skoneczny, M., Rytka, J., Maintenance of the peroxisomal compartment in glucose-repressed and anaerobically grown *Saccharomyces cerevisiae* cells. *Biochemie* 1996, **78**, 95–102.
- [25] DeLuna, A., Avendano, A., Reigo, L., Gonzalez, A., NADP-glutamate dehydrogenase isoenzymes of *Saccharomyces*

- cerevisiae*. Purification, kinetic properties, and physiological roles. *J. Biol. Chem.* 2001, *276*, 43775–43783.
- [26] Gurr, S. J., Hawkins, A. R., Drinas, C., Kinghorn, J. R., Isolation and identification of the *Aspergillus nidulans* *gdhA* gene encoding NADP-linked glutamate dehydrogenase. *Curr. Genet.* 1986, *203*, 761–766.
- [27] Nissim, I., Horyn, O., Luhovyy, B., Lazarow, A. *et al.*, Role of the glutamate dehydrogenase reaction in furnishing aspartate nitrogen for urea synthesis: Studies in perfused rat liver with <sup>15</sup>N. *Biochem. J.* 2003, *376*, 179–188.
- [28] Skopelitis, D. S., Paranychianakis, N. V., Paschalidis, K. A., Pliakonis, E. D. *et al.*, Abiotic stress generates ROS that signal expression of anionic glutamate dehydrogenases to form glutamate for proline synthesis in tobacco and grapevine. *Plant Cell* 2006, *18*, 2767–2781.
- [29] Cardoza, R. E., Maralejo, F. J., Gutierrez, S., Casqueiro, J. *et al.*, Characterization and nitrogen-source regulation at the transcriptional level of the *gdhA* gene of *Aspergillus awamori* encoding an NADP-dependent glutamate dehydrogenase. *Curr. Genet.* 1998, *34*, 50–59.
- [30] Kinghorn, J. R., Pateman, J. A., NAD and NADP L-glutamate dehydrogenase activity and ammonium regulation in *Aspergillus nidulans*. *J. Gen. Microbiol.* 1973, *78*, 39–46.
- [31] Aoki, H., Uda, I., Taguchi, K., Furuta, Y. *et al.*, The production of a new tempeh-like fermented soybean containing a high level of gamma-aminobutyric acid by anaerobic incubation with *Rizopus*. *Biosci. Biotechnol. Biochem.* 2003, *67*, 1018–1023.
- [32] Panagiotou, G., Villas-Boas, S. G., Christakopoulos, P., Nilsson, J., Olsson, L., Intracellular metabolite profilings of *Fusarium oxysporum* converting glucose to ethanol. *J. Biotechnol.* 2005, *115*, 425–434.
- [33] Panagiotou, G., Christakopoulos, P., Olsson, L., The influence of different cultivation conditions on the metabolome of *Fusarium oxysporum*. *J. Biotechnol.* 2005, *118*, 304–315.
- [34] Nosaka, K., Recent progress in understanding thiamin biosynthesis and its genetic regulation in *Saccharomyces cerevisiae*. *Appl. Microbiol. Biotechnol.* 2006, *72*, 30–40.
- [35] White, R. L., Spenser, I. D., Thiamin biosynthesis in *Saccharomyces cerevisiae*. Origin of carbon-2 of the thiazole moiety. *J. Am. Chem. Soc.* 1982, *104*, 4934–4943.
- [36] Wightman, R., Meacock, P. A., The *THI5* gene family of *Saccharomyces cerevisiae*: Distribution of homologues among the hemiascomycetes and functional redundancy in the aerobic biosynthesis of thiamin from pyridoxine. *Microbiology* 2003, *149*, 1447–1460.
- [37] Butterworth, R. F., Thiamin deficiency and brain disorders. *Nutr. Res. Rev.* 2003, *16*, 277–283.
- [38] Jordan, F., Current mechanistic understanding of thiamin diphosphate-dependent enzymatic reactions. *Nat. Prod. Rep.* 2003, *20*, 184–201.
- [39] Felenbok, B., Sequeval, D., Mathieu, M., Sibley, S. *et al.*, The ethanol regulon in *Aspergillus nidulans*: Characterization and sequence of the positive regulatory gene *alcR*. *Gene* 1988, *20*, 385–396.
- [40] Balestri, F., Giannecchini, M., Sgarrella, F., Carta, M. C. *et al.*, Purine and pyrimidine nucleosides preserve human astrocytoma cell adenylate energy charge under ischemic conditions. *Neurochem. Int.* 2007, *50*, 517–523.